Precise texture determination of the spin density wave/superconductivity mixture in the phase separation regime of (TMTSF)2 PF6

B. Salameh, P. Auban-Senzier, N. Kang, C.R. Pasquier, D. Jérome

Physica B 404 (2009) 476–478

Contents lists available at ScienceDirect

Physica B

journal homepage: www.elsevier.com/locate/physb

Precise texture determination of the spin density wave/superconductivity mixture in the phase separation regime of $(TMTSF)_2PF_6$

B. Salameh [a,b], P. Auban-Senzier [a], N. Kang [a], C.R. Pasquier [a,*], D. Jérome [a]

[a] Laboratoire de Physique des Solides, Univ. Paris-Sud, CNRS, UMR 8502, F-91405 Orsay, France
[b] Department of Applied Physics, Tafila Technical University, P.O. Box 179, Tafila 66110, Jordan

ARTICLE INFO

PACS:
74.70.Kn
74.25.Dw
74.25.Fy
74.25.Op

Keywords:
Superconductivity
Spin density waves
Phase separation

ABSTRACT

At low temperature, in a narrow range of pressure, the organic conductor $(TMTSF)_2PF_6$ exhibits a phase coexistence between two ground states, a spin density wave (SDW) state and a metallic state which presents a superconducting (SC) transition at low temperature. This phase coexistence regime extends from 6.7 kbar up to 9.5 kbar. From resistivity measurements performed along the three crystallographic a-, b'- and c^*-axes, we are able to extract an image of the evolution of the texture of $(TMTSF)_2PF_6$ in its phase coexistence regime at low temperatures: at low SC concentration, SC regions form bubbles mostly extended along the c^*-axis. Upon increasing the pressure, these bubbles extend to filaments along the c^*-axis which then stacks to form slabs perpendicular to the a-axis in agreement with theoretical work on the formation of solitons in an SDW system.

1. Introduction

Phase separation is now a common feature in strongly correlated materials: cuprates [1], manganites [2] and other various oxides. In molecular conductors, only few experimental work has been obtained. Here, the coexistence of metallic (superconducting, SC) and insulating phases may occur according to various mechanisms: first, a microscopic phase coexistence leads to the formation of stripes, this has been predicted as the situation in the so-called charge ordered state where charge disproportionation occurs [3]. Second, mesoscopic phase separation due to crystallographic instabilities related to anion ordering may occur in $(TMTSF)_2ReO_4$ [4] or $(TMTSF)_2ClO_4$ [5]. Finally, the situation of the coexistence of two electronic orders i.e. spin density wave (SDW) state and SC state is a quite unique situation. Even if a lot of work has been done in $(TMTSF)_2PF_6$ and the formation of slabs has been suggested by various experiments [6–8], its precise determination is still missing and the transition from uniform states to the slab geometry is still unknown.

In the following, we will present the evolution of this texture with respect to hydrostatic pressure. From the anisotropy measurements, we can deduce the texture formed by SDW or SC slabs at intermediate concentration of SDW or SC phases and the formation of SC filaments along c^* at low SC concentration.

2. Experiments

We have performed resistivity measurements along the three main crystallographic axis, a, b' and c^* on three different samples with the contact geometries adapted for each current configuration. In these materials, the stacking of the molecules is along a, leading to a largest conductivity along this direction in any homogeneous phase that is metallic or insulating. On the opposite, the c^*-direction is the worst conducting direction in homogeneous phases, whereas the b'-direction is the usually intermediate direction for conduction. For each sample, the applied current was chosen as the lowest possible so that the electric field along the sample remains below the depinning field in the SDW state and the voltage is far below the SC gap in the SC state. In this respect, differential resistance measurements (not shown) were systematically performed to check the regime of conduction.

3. Results and discussion

Fig. 1 presents the evolution of the resistivity along the a-axis at different applied pressures. At the lowest pressure, $p = 7.65$ kbar, the resistivity is increasing upon cooling below the SDW transition, whereas, at the highest pressures, the resistivity presents a monotonic decrease with a sharp SC transition at $T_c = 1.1$ K. At intermediate pressures, the resistivity presents the signature of both SDW and SC phases while the SC critical temperature is pressure independent. Moreover, below

* Corresponding author.
E-mail address: pasquier@lps.u-psud.fr (C.R. Pasquier).

0921-4526/$ - see front matter © 2008 Elsevier B.V. All rights reserved.
doi:10.1016/j.physb.2008.11.061

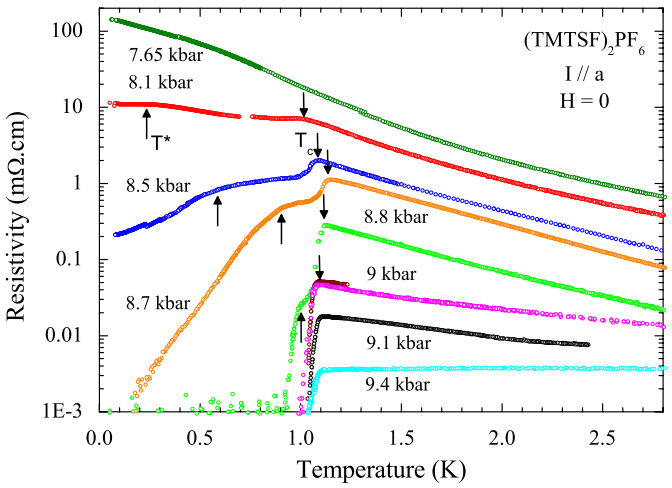

Fig. 1. Resistivity of $(TMTSF)_2PF_6$ versus temperature for different applied pressures. The current is applied along a-axis. For each pressure, the downward arrow indicates the temperature defined as the critical temperature and the upward arrow indicates the value of T^* defined in the text.

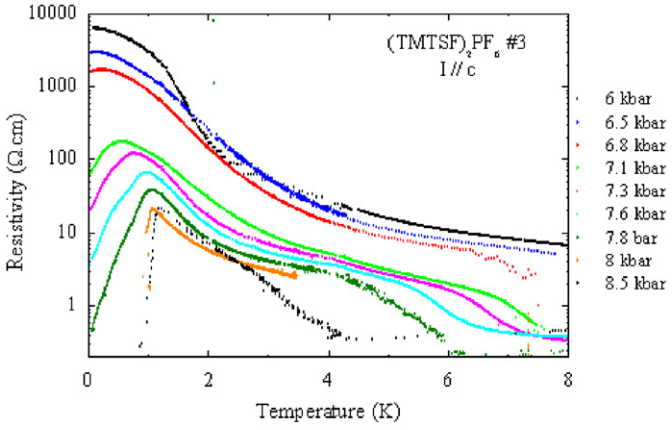

Fig. 2. Resistivity of $(TMTSF)_2PF_6$ versus temperature for different applied pressures. The current is applied along c^*-axis.

9 kbar, below the first SC transition at T_c, samples show another step on the $\rho_a(T)$ curve and a tail at the lowest temperature, the kink temperature T^* moves toward low temperature upon decreasing pressure. Such kink in the SC transition is usually associated to inhomogeneous phases in the sample so the presence of Josephson or tunnel junctions. Such behavior has been observed in all measured samples of various batches so that we can exclude extrinsic origin for these kinks. Fig. 2 presents the evolution of the resistivity along the c^*-axis at different applied pressures. Below $p = 6.8$ kbar, no decrease or plateau of the resistivity is observed at the lowest temperatures. From $p = 6.8$ to 7.8 kbar, at a critical temperature, T_c, the resistivity reaches a maximum, and for lower temperature there is a pronounced downturn where resistivity decreases with decreasing temperature. We will define the temperature T_c as the critical temperature for superconductivity, which shifts to higher temperature upon increasing pressure. Above 8 kbar, the critical temperature for superconductivity, T_c, remains nearly pressure independent. A better comparison of ρ_a and ρ_c data is shown in Fig. 3 at $p \approx 7.2$ kbar. A strong decrease in the anisotropy of the material is clearly visible upon cooling below the SDW transition temperature from about 10^5 at this temperature down to nearly 100 at $T = 50$ mK.

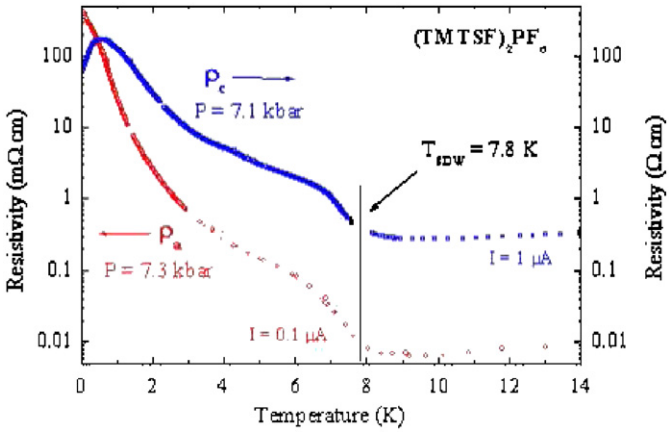

Fig. 3. Comparison of the resistivity of $(TMTSF)_2PF_6$ for two similar pressures measured along a- and c^*-axes.

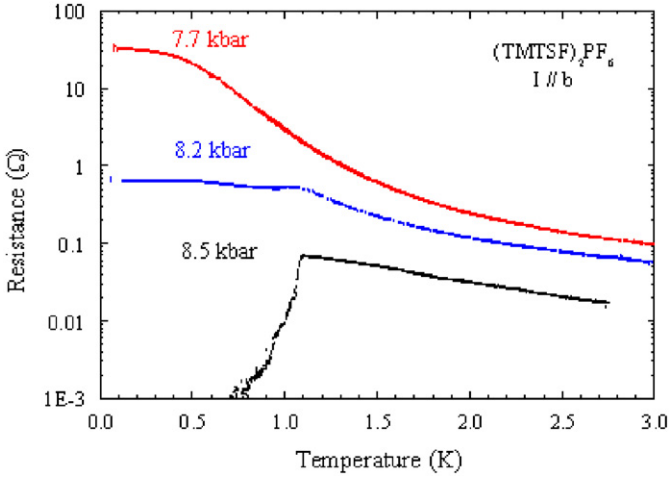

Fig. 4. Resistance of $(TMTSF)_2PF_6$ versus temperature for different applied pressures. The current is applied along b'-axis.

Finally, Fig. 4 presents few curves of the transport properties along b'-axis in the SDW/SC coexistence regime. As expected, this direction presents intermediate properties between a and c^*. Concerning the SC transition, a SC transition is visible only above 8 kbar similarly to the a-direction. However, at $p = 7.7$ kbar, the low temperature plateau differs from observation along the a-axis and suggests a better conduction along b' than along a. To summarize the data, a phase diagram is shown in Fig. 5 which is similar to the one published in Ref. [6] but provides additional data points at the lowest pressures thanks to ρ_c measurements.

The previous observations seem counterintuitive for $(TMTSF)_2PF_6$ which is known to be a strongly one-dimensional system with a best conductivity along a-axis and the poorest conductivity along c^*-axis. Above the SDW transition temperature, this is indeed observed. However, at ultra low temperatures, we observe the opposite behavior. In this respect, the measurements at $p = 8.5$ kbar are the clearest demonstration and even a weak possible error in the pressure determination does not change drastically the conclusions. Along the a-axis (Fig. 1), a very broad SC transition is observed and the resistance never reaches the zero resistance state. Along the b'-axis (Fig. 4), the SC transition is still broad but the zero resistance state is obtained below 0.7 K. Finally, a sharp resistance drop is observed along the c^*-axis (Fig. 2). Therefore, at $p = 8.5$ kbar we can conclude that SC domains extend along the c^*-axis from one side of the sample to the other. The extension of the domains along b'-axis is quite large as a zero

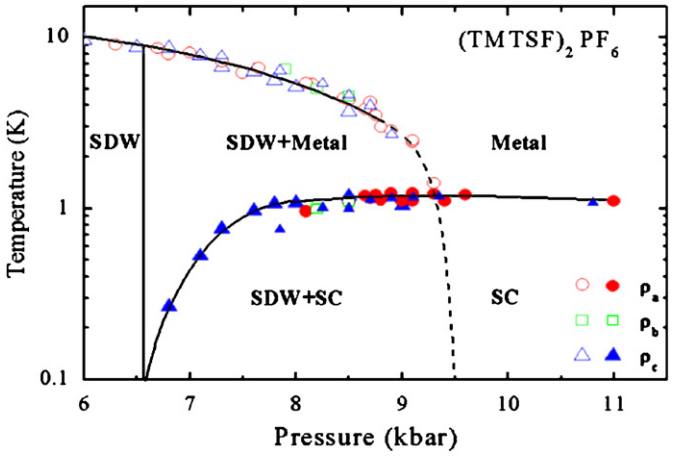

Fig. 5. Phase diagram of $(TMTSF)_2PF_6$ at low temperatures between 6 and 11 kbar. Circles denote critical temperatures extracted from ρ_a data, squares from ρ_b data and triangles from ρ_c data.

resistance state is achieved along this direction at low temperature. The broadness of the transition suggests, however, that in fact the domains are Josephson coupled along this direction. The resistivity along a-axis presents a sharp drop at T_c which we attribute to the transition of the domains. However, the absence of a true zero resistance state indicates the presence of insulating (SDW) domains in series with the SC domains. As a result, at $p = 8.5$ kbar, SC filaments extend along the c^*-axis and are strongly coupled along the b'-axis. For each pressure, the comparison of the resistivity data along the three crystallographic axes allows us to extract a qualitative image of the texture so its precise evolution with pressure.

The evolution of the texture is then the following starting from the lowest pressures. Below $p_0 = 6.6$ kbar, no decrease of the resistivity at the lowest temperatures is observed so that we can consider that we are in front of an homogeneous SDW state. From p_0 to $p_1 = 8$ kbar, even at the lowest temperature measured, $\rho_a \neq 0$, $\rho_b \neq 0$ and $\rho_c \neq 0$, but ρ_c is the only component of the tensor which presents a strong decrease of the resistivity at low temperature suggesting the presence of superconductivity. Therefore, in this regime, the SC domains are made of bubbles essentially elongated along the c^*-axis with very weak transverse dimensions along the other crystallographic axes. Between p_1 and $p_2 = 8.5$ kbar, $\rho_c = 0$, $\rho_a \neq 0$ and $\rho_b \neq 0$, SC filaments extend from one end of the sample to the other along the c^*-axis. These filaments start to aggregate along the b'-direction as ρ_b is the next component of the tensor that is reaching zero. From p_2 to $p_3 = 8.7$ kbar, $\rho_c = \rho_b = 0$, ρ_a never reaches zero at the lowest measured temperature. We are in front of slabs perpendicular to the a-axis. The rapid drop of ρ_a at T_c corresponds to the SC transition of these metallic slabs. The evolution of the residual resistance below T_c maps the evolution of dissipative SDW insulating domains between the SC slabs. From p_3 to $p_4 = 9.0$ kbar, $\rho_c = \rho_b = 0$, ρ_a reaches zero at a temperature below T_c increasing rapidly with pressure (see Fig. 1). In this narrow regime of pressure, the SC domains are sufficiently large and the distance between them is smaller than the coherence length along the a-direction, ξ_a, so that Josephson junctions are connected in series, in which $\rho_a(T)$ curves should show multiple steps. From p_4 to $p_c = 9.43$ kbar [6], $\rho_a = \rho_b = \rho_c = 0$, the existence of SDW domains is visible only above T_c by the increase of the resistance upon cooling. It is highly probable that SC and SDW slabs are still present but the Josephson coupling between the SC domains is strong. However, since SDW domains are insulating, it is impossible to estimate the shape of these domains when the SDW state is the minority phase, but by symmetry, it is highly plausible that there will be filaments or bubbles depending on the SDW concentration. For a pressure larger than p_c, we can consider that the sample is an homogeneous SC state.

Our results agree with previous demonstration of the presence of alternating SDW and SC slabs [7]. The final question is to understand why these slabs extend perpendicularly to the most conducting axis. In Ref. [6], a proposal was made of domains elongated parallel to the most conducting axis which is consistent with our recent observation in $(TMTSF)_2ReO_4$ [4] but in contradiction with the present data. On the other hand, Brazovskii et al. [9] suggested that the metallic domains are stabilized at the domain walls of the SDW domains. Indeed, considering a purely one-dimensional SDW chain, the formation of a soliton along this chain makes a defect in the magnetic structure. At the domain wall, the magnetic order parameter cancels and a metallic region can be present which could eventually present an SC transition at low temperature. Therefore, we believe that this model proposed 25 years ago is adequate to understand qualitatively the evolution of the texture with the applied pressure and the counterintuitive result of the formation of slabs perpendicular to the most conducting regions. However, further work is needed to understand the correlation of the solitons along the c-axis which seems to interact attractively like pancake vortices in a lamellar superconductor to form a 3D vortex.

In conclusion, we have presented resistivity measurements along the three different crystallographic axes in the SDW/SC coexistence regime of $(TMTSF)_2PF_6$. We establish the formation of slabs perpendicular to the most conducting axis in agreement with theoretical work on the formation of solitons in a SDW system.

Acknowledgments

This work is supported by the European Community under Grant COMEPHS No. NMPT4-CT-2005-517039. N.K. and B.S. also acknowledge this grant for financial support.

References

[1] Y. Ando, K. Segawa, S. Komiya, A.N. Lavrov, Phys. Rev. Lett. 88 (2002) 137005.
[2] E. Dagotto, T. Hotta, A. Moreo, Phys. Rep. 344 (2001) 1.
[3] H. Seo, C. Hotta, H. Fukuyama, Chem. Rev. 104 (2004) 5005.
[4] C. Colin, P. Auban-Senzier, C.R. Pasquier, K. Bechgaard, European Phys. Lett. 75 (2006) 301.
[5] H. Schwenk, K. Andres, F. Wudl, Phys. Rev. B 29 (1984) 500.
[6] T. Vuletić, P. Auban-Senzier, C. Pasquier, S. Tomić, D. Jérome, M. Héritier, K. Bechgaard, European Phys. J. B 25 (2002) 319.
[7] I.J. Lee, M.J. Naughton, P.M. Chaikin, Phys. Rev. Lett. 88 (2002) 207002.
[8] A.V. Kornilov, V.M. Pudalov, Y. Kitaoka, K. Ishida, G.-Q. Zheng, T. Mito, J.S. Qualls, Phys. Rev. B 69 (2004) 224404.
[9] S. Brazovskii, L.P. Gorkov, A.G. Lebed, Sov. Phys. JETP 56 (1982) 683.